Efficient Surface Grafting of Luminescent Silicon Quantum Dots by Photoinitiated Hydrosilylation

Fengjun Hua, Mark T. Swihart, and Eli Ruckenstein*

Department of Chemical and Biological Engineering, The University at Buffalo (SUNY), Buffalo, New York 14260-4200

Received April 8, 2005. In Final Form: April 22, 2005

We suggest a method for efficient (high-coverage) grafting of organic molecules onto photoluminescent silicon nanoparticles. High coverage grafting was enabled by use of a modified etching process that produces a hydrogen-terminated surface on the nanoparticles with very little residual oxygen and by carefully excluding oxygen during the grafting process. It had not previously been possible to produce such a clean H-terminated surface on free silicon nanoparticles or, subsequently, to produce grafted particles without significant surface oxygen. This allowed us to (1) prepare air-stable green-emitting silicon nanoparticles, (2) prepare stable dispersions of grafted silicon nanoparticles in a variety of organic solvents from which particles can readily be precipitated by addition of nonsolvent, dried, and redispersed, (3) separate these nanoparticles by size (and therefore emission color) using conventional chromatographic methods, (4) protect the particles from chemical attack and photoluminescence quenching, and (5) provide functional groups on the particle surface for further derivatization. We also show, using ^{1}H NMR, that the photoinitiated hydrosilylation reaction does not specifically graft the terminal carbon atom to the surface but that attachment at both the first and second atom occurs.

Introduction

Light emission from silicon has been a topic of intense research interest due to its potential use in displays, general illumination, and the integration of optoelectronics with silicon technology.[1] Most of this research has been carried out on porous silicon (PSi). However, it is now well understood that visible photoluminescence (PL) from PSi arises from silicon nanocrystals within it.[2] For many applications, well-characterized discrete nanocrystals would be much more useful than PSi. In silicon nanocrystals less than about 5 nm in diameter, quantum confinement widens the band gap, leading to particle size dependence of the PL wavelength, from blue to the near-infrared. Finite size effects also increase the probability of radiative recombination of excitons and decrease the possibility of nonradiative recombination.[2] Both nonradiative and radiative recombination may occur at the nanocrystal surface as well as within the nanocrystal. In particular, oxygen at the surface may introduce states within the band gap that lead to loss of emission or red-shifted emission.[3]

A wide range of applications, from bioimaging to hybrid inorganic/organic light emitters, are being pursued for discrete luminescent nanocrystals (quantum dots) of semiconductors, most notably CdS and CdSe, for which high-quality nanocrystals are readily produced as colloidal dispersions. If silicon nanoparticles of comparable quantity and quality could readily be prepared, they would have tremendous advantages in many of these applications, including (1) low toxicity, (2) emission across the entire visible spectrum from a single material, (3) compatibility with silicon microelectronics, and (4) the capability of silicon to form covalent bonds with carbon and thereby integrate inorganic and organic components at the molecular level. In this paper, we suggest steps toward the goal of producing macroscopic quantities of high-quality silicon nanoparticles as colloidal dispersions. Several methods have been developed for preparing luminescent silicon nanoparticles outside of porous silicon, including fracturing of porous silicon by ultrasonication,[4,5] inverse micellar growth,[6] laser ablation,[7,8] thermal decomposition of organosilane precursors in supercritical solvents,[9,10] solution phase methods,[11−14] plasma decomposition of silane,[15,16] and vapor phase thermal decomposition of silane or disilane.[17−19] However, two major barriers have prevented the further investigation and application of free silicon nanoparticles: lack of stability of the PL properties

* To whom correspondence should be addressed. E-mail: feaeliru@buffalo.edu.

(1) *Light Emission in Silicon From Physics to Devices*; Lockwood, D. J., Ed.; Academic Press: New York, 1998.
(2) Nirmal, M.; Brus, L. *Acc. Chem. Res.* **1999**, *32*, 407.
(3) Wolkin, M. V.; Jorne, J.; Fauchet, P. M.; Allan, G.; Delarue, C. *Phys. Rev. Lett.* **1999**, *82*, 197.
(4) Belomoin, G.; Therrien, J.; Smith, A.; Rao, S.; Twesten, R.; Chaieb, S.; Nayfeh, M. H.; Wagner, L.; Mitas, L. *Appl. Phys. Lett.* **2002**, *80*, 841.
(5) Yamani, Z.; Ashhab, S.; Nayfeh, A.; Thompson, W. H.; Nayfeh, M. *J. Appl. Phys.* **1998**, *83*, 3929.
(6) Wilcoxon, J. P.; Samara, G. A.; Provencio, P. N. *Phys. Rev. B* **1999**, *60*, 2704.
(7) Carlisle, J. A.; Dongol, M.; Germanenko, I. N.; Pithawalla, Y. B.; El-Shall, M. S. *Chem. Phys. Lett.* **2000**, *326*, 335.
(8) Carlisle, J. A.; Germanenko, I. N.; Pithawalla, Y. B.; El-Shall, M. S. *J. Electron Spectrosc.* **2001**, *114−116*, 229.
(9) English, D. S.; Pell, L. E.; Yu, Z. H.; Barbara, P. F.; Korgel, B. A. *Nano Lett.* **2002**, *2*, 681.
(10) Holmes, J. D.; Ziegler, K. J.; Doty, R. C.; Pell, L. E.; Johnston, K. P.; Korgel, B. A. *J. Am. Chem. Soc.* **2001**, *123*, 3743.
(11) Baldwin, R. K.; Pettigrew, K. A.; Garno, J. C.; Power, P. P.; Liu, G.-y.; Kauzlarich, S. M. *J. Am. Chem. Soc.* **2002**, *124*, 1150.
(12) Baldwin, R. K.; Pettigrew, K. A.; Ratai, E.; Augustine, M. P.; Kauzlarich, S. M. *Chem. Commun.* **2002**, *17*, 1822.
(13) Bley, R. A.; Kauzlarich, S. M. *J. Am. Chem. Soc.* **1996**, *118*, 12461.
(14) Heath, J. R. *Science* **1992**, *258*, 1131.
(15) Bapat, A.; Perrey, C. R.; Campbell, S. A.; Carter, C. B.; Kortshagen, U. R. *J. Appl. Phys.* **2003**, *94*, 1969.
(16) Shen, Z.; Kim, T.; Kortshagen, U. R.; McMurry, P. H.; Campbell, S. A. *J. Appl. Phys.* **2003**, *94*, 2277.
(17) Littau, K. A.; Szajowski, P. J.; Muller, A. J.; Kortan, A. R.; Brus, L. *J. Phys. Chem.* **1993**, *97*, 1224.
(18) Schuppler, S.; Friedman, S. L.; Marcus, M. A.; Adler, D. L.; Xie, Y.-H.; Ross, F. M.; Harris, T. D.; Brown, W. L.; Chabal, Y. J.; Brus, L. E.; Citrin, P. H. *Phys. Rev. Lett.* **1994**, *72*, 2648.
(19) Wilson, W. L.; Szajowski, P. J.; Brus, L. *Science* **1993**, *262*, 1242.

10.1021/la0509394 CCC: $30.25 © 2005 American Chemical Society
Published on Web 05/26/2005

and surface state of the particles, and difficulty in producing macroscopic quantities of high-quality particles as stable colloidal dispersions.

A unique method for preparing relatively large quantities of brightly luminescent silicon nanoparticles was recently developed, in which nonluminescent, crystalline nanoparticles (~5 nm diameter) are prepared by CO_2 laser heating of SiH_4-H_2-He mixtures and are then etched with a HF/HNO_3/water mixture to reduce their size and passivate their surface.[20] By controlling the etching time and conditions, the particle luminescence can be tuned from green to the near-IR. However, the green and yellow emitting particles produced by this method are unstable in air. On time scales of minutes to hours, their emission red shifts and/or decreases in intensity due to surface oxidation. Formation of an organic monolayer by hydrosilylation is an effective means of stabilizing the surface of PSi.[21,22] Several groups have reported grafting of 1-alkenes or alkynes onto H-passivated PSi or silicon wafers.[21,23−28] We have previously extended this to discrete nanoparticles, to produce clear, stable dispersions of them in polar or nonpolar solvents, and to stabilize the PL properties of orange-emitting particles.[29−31] However, in our previous work, the particles had only partial Si−H coverage on their surface, with substantial oxygen present as well. This prevented us from producing air-stable green-emitting particles and limited the range of molecules that could be grafted to the surface. The present work overcomes these important limitations by using a modified etching procedure that generates H-terminated silicon nanoparticles with minimal surface oxygen, by carefully removing oxygen from reagents, and by excluding oxygen during the hydrosilylation reactions. These modifications to our previously reported procedure result in dramatic improvements in the surface coverage of the grafted organic molecules and, therefore, in the properties and processability of the resulting particles.

Methods and Materials

Materials. Silane (SiH_4) (electronic grade, Scott Gases), 1-pentene (Acros, 95 wt %), 1-hexene (Acros, 97 wt %), 1-octene (Acros, 99+ wt %), 1-dodecene (Acros, 94 wt %), 1-octadecene (Acros, tech, 90 wt %), 5-hexen-1-ol (Aldrich, 99 wt %), undecanol (Aldrich, 99 wt %), ethyl undecylenate (Aldrich, 97 wt %), styrene (Aldrich, 99 wt %, 15 ppm 4-*tert*-butylcatechol), vinyl acetate (Alfa Aesar, 99 wt %, stabilized with hydroquinone), triethylamine (Aldrich, 99.5 wt %), and trifluoroacetic acid (Aldrich, 99 wt %) were used as received or were degassed by a series of freeze−thaw cycles as described below. Silicon nanoparticles were prepared by silane (SiH_4) dissociation through heating with a CO_2 laser beam (Coherent, model 42, 60 W) in an aerosol reactor, as described in detail by Li et al.[20] The resulting crystalline particles, with sizes ranging from 5 to 10 nm, were collected on cellulose nitrate membrane filters. They did not exhibit photoluminescence.

Etching Procedure. The particles were etched with a mixture of HF (48 wt %) and HNO_3 (69 wt %) (10/1, v/v). 20 mg of silicon nanoparticles was dispersed via sonication into 2−6 mL of methanol. 11 mL of acid mixture was added to the resulting dispersion. The particle sizes decreased, and the particle surfaces were passivated during this etching process. As a result, the particles exhibited bright, visible photoluminescence. The color of the photoluminescence changed from red to yellow to green as the etching proceeded. The etching rate decreased with increasing amount of methanol used to disperse the particles initially. When the desired emission color was reached, the etching was slowed by adding about 10 mL of methanol or a methanol/water mixture (1/3, v/v). The particles were collected on a poly(vinylidene fluoride) (PVDF) membrane filter (pore size 100 nm) and washed with a large amount of the methanol/water mixture to remove any adsorbed acid mixture. Finally, the particles were rinsed with pure methanol.

Photoinitiated Hydrosilylation. The freshly etched particles (6 mg of red emitting particles, 3 mg of yellow emitting particles, or 1.5 mg of green emitting particles) were transferred into a 25 mL Aldrich Schlenk-type reactor containing a magnetic stirrer and 2 mL of the compound that was to be attached to the particles. Sonication was used to disperse the particles, but a stable colloidal dispersion was not formed and the reactor contents appeared cloudy in all cases. The reactor was attached to a high-vacuum line, and the contents were degassed using at least three freeze−thaw cycles. A Rayonet photochemical reactor (Southern New England Ultraviolet Co.) equipped with 10 RPR-2537 Å UV tubes was used to initiate the hydrosilylation reaction. The reaction time required varied substantially depending on the compound being attached to the particles and the particle size, as discussed further below. After reaction, a clear dispersion was obtained. It was drawn through a PTFE syringe filter (pore size 0.45 nm). For the relatively volatile compounds (1-pentene, 1-hexene, 1-octene, styrene, or vinyl acetate), the excess monomer was removed under vacuum on a rotary evaporator at room temperature. The excess of 1-dodecene or 5-hexen-1-ol was removed under vacuum at 60 °C and of 1-octadecene, undecanol, or ethyl undecylenate in a vacuum oven at 90 °C. Styrene-grafted and vinyl acetate-grafted particles were further purified by passing the dispersion through an inhibitor remover (Aldrich, part numbers 30632-0 and 30631-2, respectively, to remove *tert*-butyl catechol and hydroquinone, respectively) using THF as the solvent.

Size Separation Using Column Chromatography. The ethyl undecylenate-grafted silicon particles were dispersed in THF (20 mg/mL) and introduced into a silica gel column (Aldrich, 200−400 mesh). Size separation was carried out with a 2 to 1 (v/v) mixture of cyclohexane and THF as the mobile phase. The fractions exhibiting emission of different colors were collected, and the solvents were removed using a rotary evaporator.

Characterization. Fourier transform infrared (FTIR) spectra for etched silicon and grafted particles were examined using a Mattson Galaxy Series 5000 FTIR spectrometer. IR spectra of the etched Si nanoparticle powders were obtained in transmission after mixing the particles with KBr and pressing the mixture into pellets. The spectra of the grafted silicon particles were measured in the horizontal attenuated reflectance (ATR) mode by casting a drop (chloroform solution) on the internal reflection element card. For studying the stability of the organic monolayer upon exposure to heat, UV illumination, and basic conditions by FTIR, the particles were first deposited on the internal reflection element card, and then spectra were measured before and after periods of exposure to heat, light, or basic solutions. Proton NMR and UV absorption were carried out on a 400 MHz INOVA-400 and a Thermo Spectronic Genesys-6, respectively.

Transmission electron micrographs (TEM) of the etched silicon and grafted silicon particles were obtained using a JEOL JEM 2010 microscope at an acceleration voltage of 200 kV in the bright field image mode. Etched silicon powders were prepared for imaging by dispersing them in methanol and evaporating multiple drops of this dispersion onto an ultrathin carbon-coated copper grid. Similarly, samples of the grafted silicon particles were dispersed in toluene or cyclohexane overnight and then dropped onto an ultrathin carbon-coated copper TEM grid.

(20) Li, X.; He, Y.; Talukdar, S. S.; Swihart, M. T. *Langmuir* **2003**, *19*, 8490.
(21) Buriak, J. M. *Chem. Rev.* **2002**, *102*, 1271.
(22) Waltenburg, H. N.; Yates, J. *Chem. Rev.* **1995**, *95*, 1589.
(23) Linford, M. R.; Chidsey, C. E. D. *J. Am. Chem. Soc.* **1993**, *115*, 12631.
(24) Linford, M. R.; Fenter, P.; Eisenberger, P. M.; Chidsey, C. E. D. *J. Am. Chem. Soc.* **1995**, *117*, 3145.
(25) Boukherroub, R.; Wayner, D. D. M. *J. Am. Chem. Soc.* **1999**, *121*, 11513.
(26) Buriak, J. M.; Stewart, M. P.; Geders, T. W.; Allen, M. J.; Choi, H. C.; Smith, J.; Raftery, D.; Canham, L. T. *J. Am. Chem. Soc.* **1999**, *121*, 11491.
(27) Buriak, J. M.; Allen, M. J. *J. Lumin.* **1999**, *80*, 29.
(28) Buriak, J. M.; Allen, M. J. *J. Am. Chem. Soc.* **1998**, *120*, 1339.
(29) Li, Z. F.; Ruckenstein, E. *Nano Lett.* **2004**, *4*, 1463.
(30) Ruckenstein, E.; Li, Z. F. *Adv. Colloid Interface Sci.* **2005**, *113*, 43.
(31) Li, X.; He, Y.; Swihart, M. T. *Langmuir* **2004**, *20*, 4720.

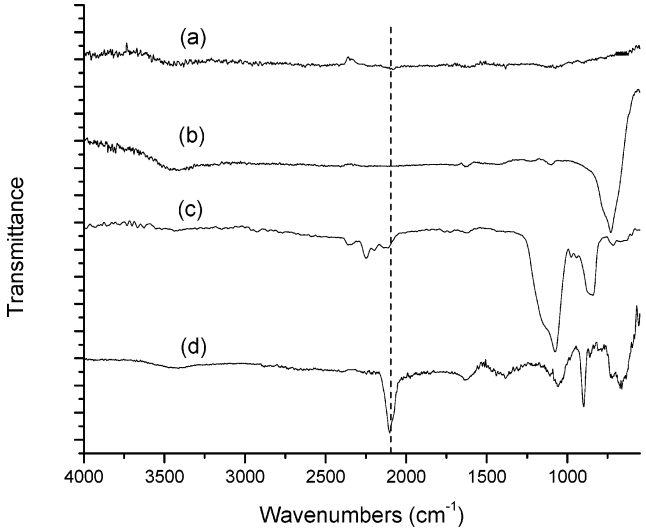

Figure 1. FTIR spectra of silicon particles in KBr pellets: (a) unetched silicon particles, (b) after etching with mixture of HF (48 wt %)/HNO_3 (69 wt %) (10/1, v/v) and then washing with methanol, (c) after etching with a solution containing 3 wt % HF and 30 wt % HNO_3 and then washing with water, (d) after etching with HF (48 wt %)/HNO_3 (69 wt %) (10/1, v/v) and then washing with methanol/water (3/1, v/v).

The powder XRD spectra of the etched silicon particles were recorded on a SIEMENS, D500, X-ray diffractometer, operated at 30 MA and 40 $kV_{P\ MAX}$. The grafted silicon particles were first dissolved in chloroform and placed on a glass plate. After evaporating the solvent, a film was formed on the plate, and this supported film was used for the measurement.

Photoluminescence (PL) spectra were recorded using a SLM model 8100 spectrofluorimeter with a 385 or 425 nm emission cutoff filter. The excitation wavelength was set at 310 nm and the emission scanned from 400 to 900 nm. Solution samples of grafted silicon particles were prepared at a concentration of about 0.01 g/L, filtered through a syringe filter (PTFE, pore size 450 nm), and then introduced into a quartz cuvette. Solid film samples were prepared by dropping the sample solution onto a quartz plate followed by evaporation of the solvent. PL quenching experiments were performed by adding 50 μL of triethylamine to 3 mL aliquots of each dispersion. After mixing 3 min to allow the system to reach equilibrium, the PL spectrum was recorded. Following this, 200 μL of trifluoroacetic acid (TFA) was added, and the PL was again determined after mixing.

The differential scanning calorimetery (DSC, Perkin-Elmer, DSC-7) of the grafted silicon particles was carried out using a heating rate of 10 °C/min from −50 to 200 °C. The thermogravimetric analysis (TGA) of the grafted particles was performed using a Du Pont Thermal Analyst 2000 module from 20 to 900 °C at a heating rate of 15 °C/min.

Results and Discussion

Improved Particle Etching Procedure. The first advance described here is an improved etching procedure that produces silicon nanoparticles with bright photoluminescence ranging from red to green, with a remarkably high density of hydrogen and low density of oxygen on their surface. Particles produced by laser heating of silane were first etched with a mixture of concentrated HF (48 wt %) and HNO_3 (69 wt %) (10/1, v/v). The FTIR spectrum from particles washed with pure methanol after etching is shown in Figure 1b. This spectrum exhibits a single broad peak near 760 cm^{-1}, which we tentatively assign to $Si-F_x$ stretching. While it is well established that HF etching of silicon wafers results in H-termination,[32] it is also clear that the etching chemistry for these nanoparticles differs significantly from that of bulk silicon. For example, the etching rate is orders of magnitude slower for the same etchant concentrations (less than 1 nm/min for the nanoparticles vs μm/min for a silicon wafer). The IR spectrum of SiF_x on a surface is not well established, but for $(CH_3)_3SiSiF_3$ and F_3SiSiF_3, the SiF_3 symmetric stretch is at 815 and 824 cm^{-1}, respectively.[33,34] In going from these small molecules to a surface (of effectively infinite mass) a shift of the absorption to lower frequency is expected. Thus, fluorine termination, though unexpected, seems the most likely interpretation of the spectrum in Figure 1b. In any case, the particle surface after etching and washing with methanol was highly reactive toward water. Subsequent treatment with a 3:1 (v/v) water/methanol mixture resulted in a hydrogen-passivated surface, as demonstrated by the FTIR spectrum in Figure 1d, where the strong absorption at 2105 cm^{-1} is characteristic of $Si-H_x$ stretching. The very weak absorption at 1087 cm^{-1}, which can be assigned to Si−O stretching, demonstrates that very little oxygen is present. This contrasts sharply with previous work in which the particles were etched under oxidizing conditions, using a HF to HNO_3 ratio that was lower than that used here by a factor of about 70.[20,31] Under those conditions of relatively high HNO_3 and low HF concentration, a substantial amount of oxygen was always present on the particle surface after etching. A typical FTIR spectrum of particles etched under those conditions is included in Figure 1c for comparison. Even further treatment with various concentrations of HF alone did not lead to complete removal of oxygen from the surface[31] after etching with high HNO_3 and low HF concentrations. It should be noted here that both the HF to HNO_3 ratio used in the etching and the 3:1 (v/v) water-to-methanol ratio used to treat the particles after etching were essential to minimizing oxygen incorporation on the particle surface. Significant deviations in either direction from the 3:1 (v/v) ratio of water to methanol, substitution of ethanol for methanol, and other variations in the procedure all led to significant oxygen incorporation on the particle surface. Figure S1 in the Supporting Information shows the largely oxygen-terminated surface formed when the particles were washed with pure water after etching.

With the improved procedure using high HF concentrations, luminescent silicon particles displaying green to red emission were readily prepared by varying the ratio of etchant solution to unetched particles and the etching time. The yield of etched particles (fraction of the particle mass before etching that remained after etching) was significantly higher (typically >50% for red-emitting particles) than that obtained using the previous method. High-resolution TEM images showed small crystalline domains in red-emitting (~5 nm domains), yellow-emitting (~3 nm domains), and green-emitting (<3 nm domains) samples (see Supporting Information, Figure S2), but it was not possible to obtain quantitative size distributions from the images. Powder XRD spectra for the yellow- and red-emitting particles showed the three characteristic diffraction peaks for silicon at 28.4°, 47.5°, and 56.3°, but these peaks were not resolvable for the green-emitting particles (see Supporting Information, Figure S3).

Photooxidation of Etched Particles. Green-emitting particles were rapidly photooxidized in air when illuminated with 355 nm light. Under ordinary room

(32) Higashi, G. S.; Chabal, Y. J.; Trucks, G. W.; Raghavachari, K. *Appl. Phys. Lett.* **1990**, *56*, 656.
(33) Xue, Y.; Xu, X.; Xie, D.; Yan, G. *J. Mol. Struct. (THEOCHEM)* **1999**, *469*, 151.
(34) Zink, R.; Hassler, K. *Spectrochim. Acta, Part A* **1999**, *55*, 333.

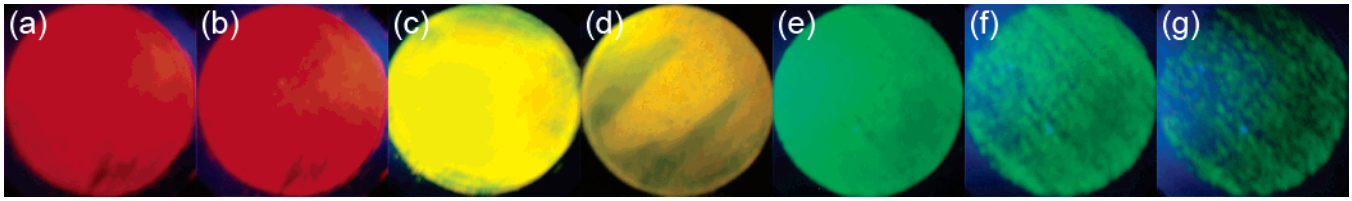

Figure 2. Photooxidation of particles under 355 nm UV excitation in air. Red-emitting particles (a) initially and (b) after 10 min illumination. Yellow-emitting particles (c) initially and (d) after 3 min illumination. Green-emitting particles (e) initially, (f) after 20 s illumination, and (g) after 40 s illumination.

Scheme 1. Attachment of Molecules with a Terminal Double Bond to H-Terminated Silicon Particles via Hydrosilylation

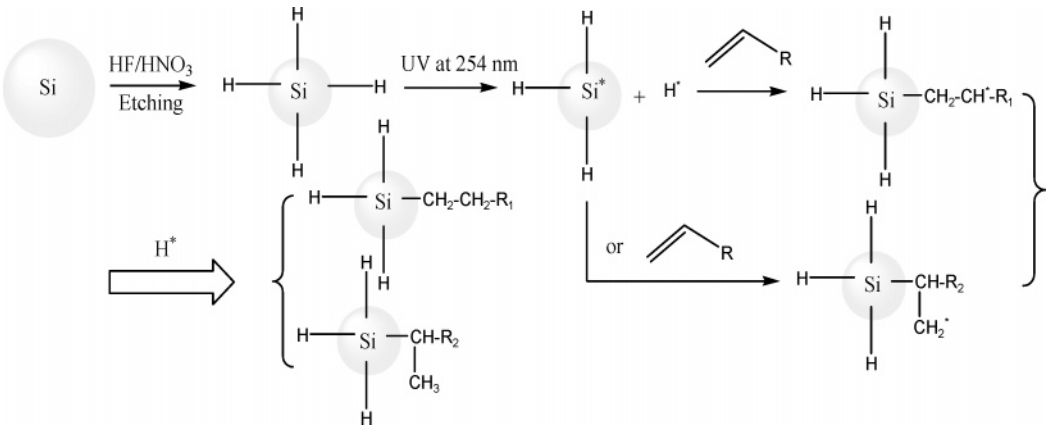

illumination in air, they lost their PL on time scales of minutes to hours. However, in a nitrogen-filled glovebox under the same conditions they were stable indefinitely. The photoluminescence of yellow-emitting particles was also degraded by photooxidation, but much more slowly than that of green-emitting particles. Photoluminescence from red-emitting particles was not rapidly degraded by photooxidation. This is illustrated in Figure 2.

Grafting of Organic Molecules onto Silicon Nanoparticles. Photoinitiated hydrosilylation was carried out in a UV reactor using several compounds that each contained a terminal double bond, as illustrated in Scheme 1. Removal of dissolved oxygen from the reagents, by several freeze−pump−thaw cycles, was essential. If the reagents were used as-received or if they were only bubbled with nitrogen to displace some of the dissolved oxygen from them, then photooxidation competed with the hydrosilylation reaction, and significant oxidation of the particle surface occurred. Figure 3 shows attenuated total reflection (ATR) FTIR spectra for orange-emitting silicon nanoparticles before and after photoinitiated hydrosilylation with various double-bond-terminated compounds (vinyl acetate, styrene, 1-dodecene, ethyl undecylenate, and 1-undecanol). The clear presence of -characteristic vibrations for each organic molecule in the particle samples after reaction, along with the reduction in Si−H intensity and the absence of peaks characteristic of the terminal double bond, indicates that the organic molecules were covalently attached to the silicon surface. Similar FTIR spectra for 1-pentene, 1-hexene, 1-octene, and 1-octadecene are included in the Supporting Information, Figure S4.

^{1}H NMR spectra from samples that had been dried and redispersed in deuterated chloroform confirmed that the monomers were attached via the expected hydrosilylation. Figure 4 shows the spectrum for 1-dodecene grafted particles. Spectra for samples grafted with other compounds are available in the Supporting Information, Figures S5 and S6. Peaks were assigned as shown in Figure 4. Those labeled a and b are at the standard positions for methyl and methylene groups, respectively, in alkenes. For the hydrogens labeled c and d, the assignment is less obvious. In molecular silanes, methyl group protons adjacent to a silicon atom exhibit a smaller chemical shift than those in alkenes. For example, in trihexylsilane, the methylene protons adjacent to the silicon atom appear at 0.58 ppm.[35] The peak position is similar in other tri- and tetraalkylsilanes. Similarly, the proton on the tertiary carbon adjacent to silicon in triisopropysilane appears at 1.07 ppm, while protons on tertiary carbons in branched alkanes typically appear at 1.5−1.8 ppm.[35] Thus, we might expect the signals from the hydrogens labeled c and d in Figure 4 to be near 0.6 and 1.1 ppm, respectively. However, the peak positions in silanes depend on the other atoms bonded to the silicon. For example, in trichlorooctadecylsilane, the methylene protons adjacent to the silicon atom appear at 1.45 ppm,[35] a somewhat higher chemical shift than methylene protons in alkanes. In this study, we consistently observed a small peak like that labeled d in Figure 4 that can be most reasonably assigned to hydrogen of the type labeled d in Figure 4 (hydrogen attached to a carbon bonded to two other carbons and the silicon nanoparticle). This peak occurs at a chemical shift typical of a hydrogen atom on a tertiary carbon in an alkene, rather than at a chemical shift typical of a hydrogen atom on a carbon bound to two other carbons and a silicon in a molecular silane. This gives indirect evidence that the hydrogens on the carbon adjacent to the silicon surface have chemical shifts closer to those of hydrogens in alkanes than hydrogens on carbons adjacent to silicon in a molecular tri- or *tert*-alkylsilane. On the basis of this observation, we have included the methylene hydrogens labeled c in Figure 4 with the other

(35) Spectral Database for Organic Compounds SDBS, National Institute of Advanced Industrial Science and Technology, http://www.aist.go.jp/RIODB/SDBS/, accessed April 20, 2005.

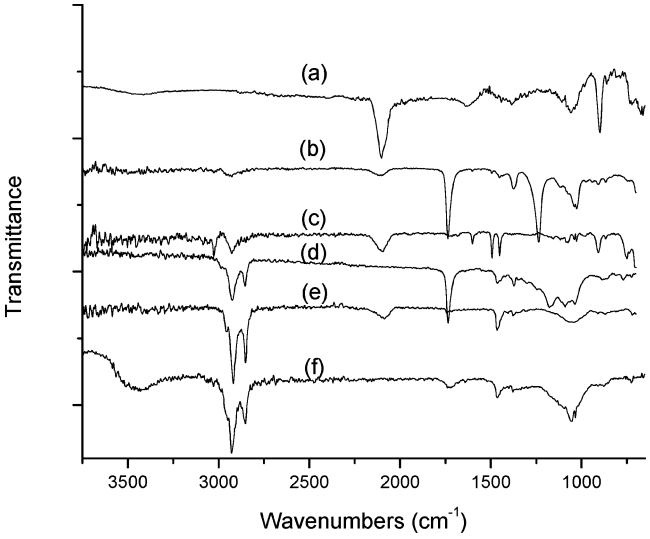

Figure 3. FTIR spectra from nanoparticles with (a) hydrogen, (b) vinyl acetate, (c) styrene, (d) ethyl undecylenate, (e) 1-dodecene, and (f) undecanol on their surface. Spectrum (a) was taken in transmission in a KBr pellet. All others were taken in attenuated total reflection (ATR) mode.

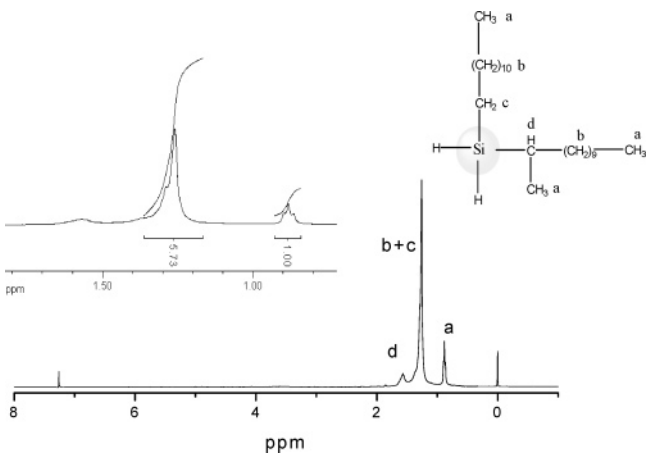

Figure 4. ^{1}H NMR spectrum of 1-dodecene-grafted silicon particles in deuterated chloroform.

methylene hydrogens at 1.3 ppm. This assignment seems to provide the most consistent explanation of all of the spectra.

In hydrosilylation reactions, it is often assumed that the monomer attaches at the terminal (alpha) carbon atom. Some catalysts can confer this specificity as well. However, in the present case, reaction at either end of the double bond is possible. Here, we observed that the selectivity toward reaction at the terminal carbon was monomer dependent, and that for small alkenes reaction at the second (beta) carbon atom was favored. The selectivity toward reaction at the terminal carbon can be roughly estimated from the area ratio between the 1.29 ppm (methylene) and 0.88 ppm (methyl) peaks in the ^{1}H NMR spectrum. For dodecene, the measured ratio of 5.73 as shown in Figure 4 corresponds to 63% of reaction occurring at the terminal carbon. If we had assumed that the methylene hydrogens adjacent to the silicon surface, labeled c in Figure 4, were contributing to the peak at 0.9 ppm, along with the methyl hydrogens rather than contributing to the peak near 1.3 ppm, then the expected area ratio of the 1.3 ppm peak to the 0.9 ppm peak would be 4 to 1 for attachment only at the alpha carbon and 3 to 1 for attachment only at the beta carbon. The observed ratio of 5.73 to 1 is significantly outside that range, further supporting the conclusion that the signal from the methylene hydrogens on the carbon adjacent to the particle appears in the 1.3 ppm peak. The appearance of the peak at 0.9 ppm for particles grafted with styrene, vinyl acetate, and 1-undecenol as shown in Figure S6 (Supporting Information) provides direct evidence of addition at the beta carbon, since in these three cases there are no methyl groups present unless grafting occurs at the beta carbon. Neither the parent molecules nor molecules grafted at the alpha carbon should give a peak at 0.9 ppm, characteristic of the methyl hydrogens. Selectivity toward reaction at the terminal carbon increased with increasing size of the linear alkenes, from 39% for 1-pentene to 64% for 1-octadecene, as summarized in Table 1. The ability to study the hydrosilylation reaction using routine solution NMR spectroscopy is a significant advantage of working with stable colloidal dispersions of particles like those used here, rather than porous silicon or silicon wafers where solution NMR is not applicable.

Thermogravimetric analysis (TGA, see Supporting Information, Figure S7) and ^{1}H NMR were used to estimate the degree of grafting of the organic molecules onto the silicon particles. This is shown in more detail in Table 1 for green-emitting nanoparticles. The mass fraction of the organic component of the grafted nanoparticles can be obtained directly from TGA, assuming that all of the organic is removed at the highest temperature and that there is no increase in mass due to silicon oxidation. It can be obtained indirectly from ^{1}H NMR by comparison of integrated peak areas from the grafted organic to those from a known quantity of tetramethylsilane (TMS) used as an internal standard. Thus, the molar ratio of grafted molecules to silicon atoms in the particle can be estimated, as shown in Table 1. The results based on TGA and ^{1}H NMR are reasonably consistent. It is more difficult to estimate the ratio of grafted molecules to surface Si atoms because of uncertainty in the particle size and, therefore, the surface-to-volume ratio of the surface. However, rough estimates can be made using the fraction of atoms on the surface of particular silicon nanoparticle structures $\approx$2 nm in diameter.[36] A compact icosohedral structure containing 280 total Si atoms has 120 surface atoms (43%), and the next-larger icosohedral structure with 600 total Si atoms has 200 surface atoms (33%). A compact bulklike structure with 323 total Si atoms has 124 surface atoms (38%). These are the most compact possible clusters in this size range, so other clusters of similar size will have a slightly larger fraction of surface atoms. The ratios of organic molecules to Si atoms shown in Table 1 are thus comparable to the expected fraction of the Si atoms that are on the surface. This suggests that a nearly complete monolayer has been formed. Table 1 illustrates that for such small particles grafted with organic molecules the overall structure can contain more organic material than silicon. This is not unreasonable. As an example, consider the compact bulklike cluster of 323 silicon atoms, which has 124 surface atoms. If one octadecene molecule (with a molecular weight of 252.5 amu) were attached to each of the 124 surface atoms, then the total octadecene mass would be 31 310 amu compared to a silicon mass of 9044 amu. Thus, by mass, the particle would be 78% octadecene and just 22% silicon. This is in reasonable agreement with the values given in Table 1 for octadecene. The situation is similar for the

(36) Zhao, Y.; Kim, Y.-H.; Du, M.-H.; Zhang, S. B. *Phys. Rev. Lett.* **2004**, *93*, 015502.

Table 1. Reaction Selectivity and Grafting Degree of Various Compounds with Green-Emitting Silicon Nanoparticles

ligand	area ratio, $A_{1.29}/A_{0.88}$ [a]	terminal carbon fraction, n[b]	mass fraction ligand, g[c,d]	mole fraction ligand, m[e]	ligand to Si atom ratio, r[f]
1-pentene	1.44	38.7	0.52 (0.51)	0.30 (0.29)	0.43 (0.42)
1-hexene	1.93	39.9	0.52 (0.53)	0.27 (0.27)	0.36 (0.38)
1-octene	3.02	45.1	0.56 (0.54)	0.24 (0.23)	0.31 (0.29)
1-dodecene	5.73	63.0	0.68 (0.67)	0.26 (0.26)	0.36 (0.34)
1-octadecene	9.05	63.9	0.83 (0.77)	0.35 (0.27)	0.53 (0.37)
styrene			0.72 (0.67)	0.40 (0.35)	0.67 (0.54)

[a] $A_{1.29}$ and $A_{0.88}$ are integral areas of ^{1}H NMR peaks at 1.29 and 0.88 ppm, which are assigned to methylene and methyl protons, respectively. [b] n is the fraction of reaction occurring at the terminal carbon, calculated from the equation $^2/_3 \times (m - 1)(n + {}^1/_3 \times (m - 3) \times (1 - n) = A_{1.29}/A_{0.88}$, where m is the chain length of the alkene. [c] Grafting degree, g, is the mass fraction of the organic component, $g = (G_0 - G_1)/G_0$, obtained from TGA, where G_0 and G_1 are the initial and the final masses, respectively. [d] Data in parentheses were estimated from ^{1}H NMR spectra using the ratio of the integrated area of peaks due to ligand hydrogens to the peak from TMS (internal standard) hydrogens, using known masses of TMS and grafted particles. [e] Ligand mole fractions were calculated from $m = (g/MW_1)/(g/MW_1 + (100 - g)/MW_2)$, where MW_1 and MW_2 are molecular weights of the ligand and Si, respectively. Data in parentheses were from NMR. [f] Computed from $r = m/(1 - m)$. Data in parentheses were from NMR.

Table 2. Qualitative Reactivity of Various Compounds with H-Terminated Luminescent Silicon Nanoparticles by Photoinitiated Hydrosilylation[a]

	green emitting	yellow emitting	red emitting
1-pentene	25		
1-hexane	30	60	
1-octene	30	45	60
1-dodecene	20	45	60
1-octadecene	30	60	120
styrene	3	5	10
vinyl acetate	20	35	
ethyl undecylenate	20	30	60
1-undecanol	60	120	180
5-hexen-1-ol	45	120	

[a] Approximate reaction time, in minutes, for the colloidal dispersion to appear clear, rather than cloudy. This is an indication that substantial attachment of the organic compound has occurred. Missing entries indicate that the solution often did not become clear for that combination of organic compound and particles.

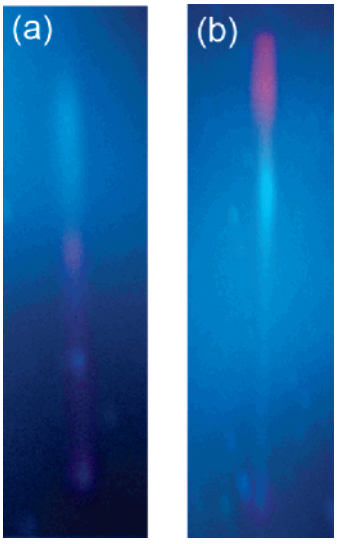

Figure 5. Size separation of nanoparticles by TLC, using (a) 2:1 and (b) 1:3 cyclohexane:THF (v/v) mixtures as the mobile phase.

other grafted molecules. For pentene, hexene, and octene, FTIR spectra taken after grafting show a small amount of residual hydrogen on the surface, so it is clear that the organic molecules have not occupied every possible surface site in those cases. However, these small particles have a substantial number of atoms that occupy edge or vertex positions where they may be able to accommodate two organic ligands or an organic ligand and a hydrogen atom.

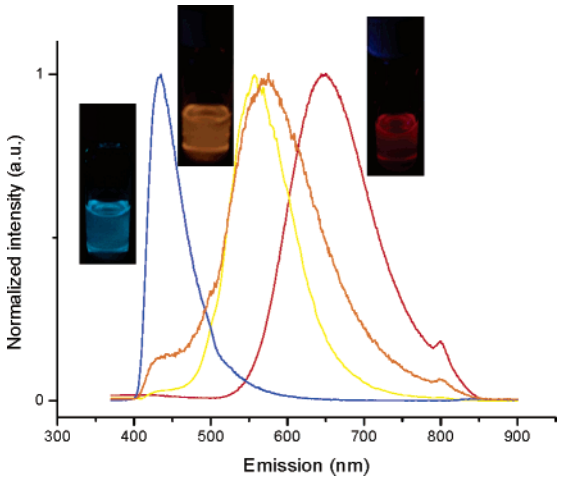

Figure 6. Normalized PL spectra of ethyl undecylenate-grafted silicon fractions separated using column chromatography. The orange spectrum is from the sample that was separated into three fractions with the blue, yellow, and red spectra. The insets are photos under 355 nm illumination.

While quantitative chemical kinetics of hydrosilylsation were beyond the scope of the present investigation, the relative reactivity of the different organic compounds with the hydrogen-terminated silicon nanoparticles was considered qualitatively. Table 2 shows the approximate reaction time required for grafting of various molecules onto silicon nanoparticles of different sizes, as estimated from the time required for the colloidal dispersion to appear clear, rather than cloudy. Required reaction times for the various alkenes and for the two esters used were similar. Styrene reacted more quickly, and the alcohols reacted more slowly. In all cases, the reaction proceeded faster on the smaller (green-emitting) particles. Since the reaction time was taken as the time when the colloidal dispersion became clear, this observation may be affected by the fact that smaller particles are more easily dispersed and might require a lower degree of grafting to form a clear dispersion. The fact that the smallest organic molecules yielded stable dispersions of smaller particles, but not larger particles, illustrates the fact that smaller particles are more easily dispersed.

Dense grafting of an organic monolayer onto the silicon nanoparticles substantially changes their chemical and physical properties. After reaction, the particles formed stable colloidal dispersions in organic solvents including THF, chloroform, toluene, DMF, and DMSO. This ability to form stable dispersions in a range of solvents and solvent mixtures enabled the chromatographic separation of particles by size. Ethyl undecylenate-grafted silicon

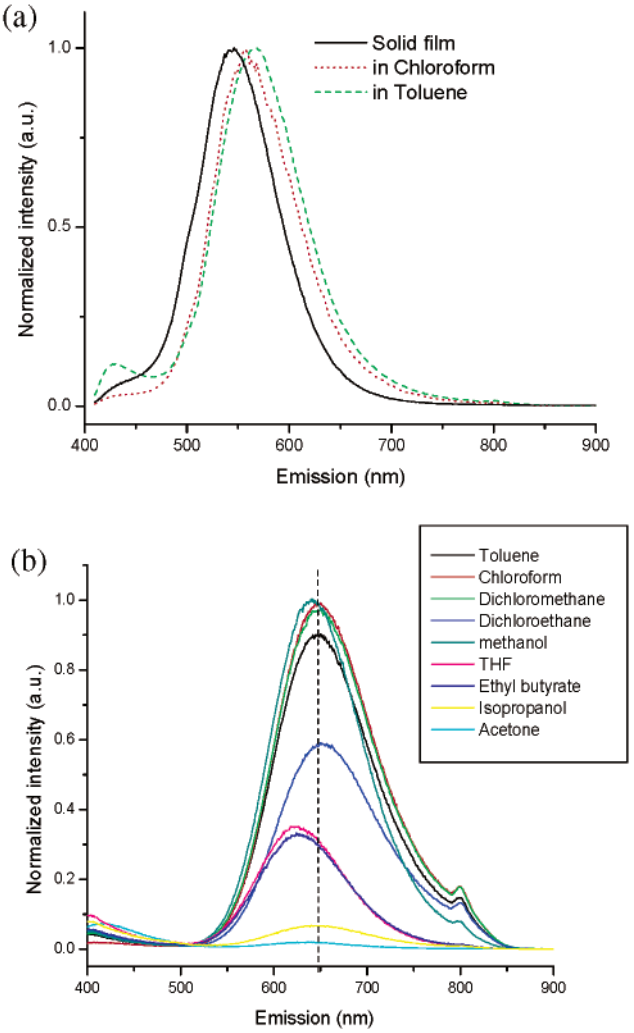

Figure 7. Effect of solvent on emission from grafted silicon nanoparticles: (a) red shift upon dispersion of dry styrene-grafted particles in solvents and (b) variation of PL with solvent for dodecene-grafted particles. Solvent changes were made by evaporation of one solvent followed by addition of a new solvent so that the concentration was the same in all measurements.

particles (orange-emitting) were size separated via conventional thin-layer chromatography (TLC) and column chromatography. Figure 5 shows photographs of TLC plates upon which the ethyl undecylenate-grafted particles were separated by size, which corresponds to separation by emission color, using different solvent mixtures as the mobile phase. As shown there, when the TLC plate was developed with a 2:1 (v/v) cyclohexane:THF mixture, the smallest (blue-emitting) particles moved further than the largest (red-emitting) particles. However, when the plate was developed with a 1:3 (v/v) cyclohexane:THF mixture, the larger particles moved further. These results can be extended to column chromatography. Figure 6 shows photographs and PL spectra for three size fractions with blue, yellow, and red emission that were obtained from an orange-emitting sample by column chromatography with a 2:1 (v/v) cyclohexane:THF mixture as the mobile phase.

Stability of the silicon particles against heat, photooxidation, chemical attack, and UV radiation was dramatically improved by the organic monolayer, and the organic monolayer itself was also quite stable. The 1-dodecene monolayer was able to withstand heating at 70 °C in air for 5 days, 30 min illumination with 254 nm UV light, 120 min illumination with 363 nm light, 15 min

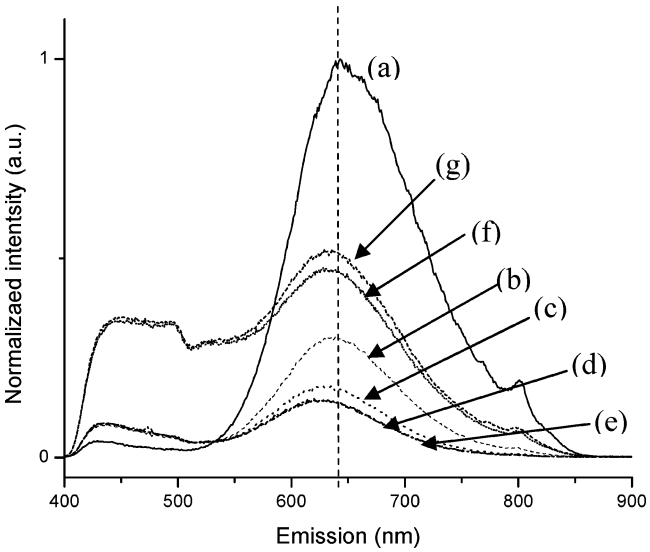

Figure 8. PL spectra of 1-dodecene-grafted silicon (0.1133 g/L) quenched by triethylamine (33 g/L) as a function as time: (a) solid line, 0 min; (b) dashed line, 5 min; (c) dotted line, 15 min; (d) dash−dot line, 20 min; (e) dash−dot−dot line, 40 min; (f) short dot, 10 min after addition of TFA (100 g/L); (g) short dash, 40 min after addition of TFA (100 g/L).

in pH = 14 solution at 70 °C, or 5 min in boiling pH = 14 solution. Some of these stability checks were also performed for styrene-grafted and ethyl undecylenate-grafted particles. FTIR spectra before and after these treatments (examples are shown in the Supporting Information, Figures S8−S15) showed that the organic monolayer remained intact after these treatments but that in most cases any residual Si−H on the surface was oxidized. In many cases, this oxidation led to a blue shift of the PL. However, the PL of grafted green-emitting particles did not disappear or red-shift upon extended exposure to air, UV illumination, or basic solutions as did the PL of untreated green-emitting particles. These stability tests were performed for solid particle deposits on the ATR element for FTIR spectroscopy, which precluded quantitative PL measurements on the same samples.

Even after surface grafting, the PL properties were sensitive to the medium surrounding the particles. When styrene-grafted silicon particles were dispersed in chloroform or toluene, a red shift of the PL was observed, as shown in Figure 7. This can be attributed to energy transfer to the solvent (solvent relaxation effect). Energy loss and PL intensity decrease could be qualitatively correlated with chemical differences between the organic monolayer and the solvent used, with the greatest effects seen for oxygen-containing compounds. However, there was no straightforward correlation between these effects and solvent dipole moment, index of refraction, dielectric constant, or orientational polarizability. Emission from grafted silicon particles was partially quenched by triethylamine, whose ability to quench emission from PSi and Si nanoparticles is well-known.[37,38] However, complete quenching was not observed, indicating that a densely grafted organic monolayer on the silicon surface can partially protect the particles against quenching by amines. Figure 8 shows typical results for quenching with triethylamine and PL recovery upon addition of trifluoroaceic acid (TFA). Additional results are included in the

(37) Sweryda-Krawiec, B.; Chandler-Henderson, R. R.; Coffer, J. L.; Rho, Y. G.; Pinizzotto, R. F. *J. Phys. Chem.* **1996**, *100*, 13776.
(38) Germanenko, I. N.; Li, S.; El-Shall, M. S. *J. Phys. Chem. B* **2001**, *105*, 59.

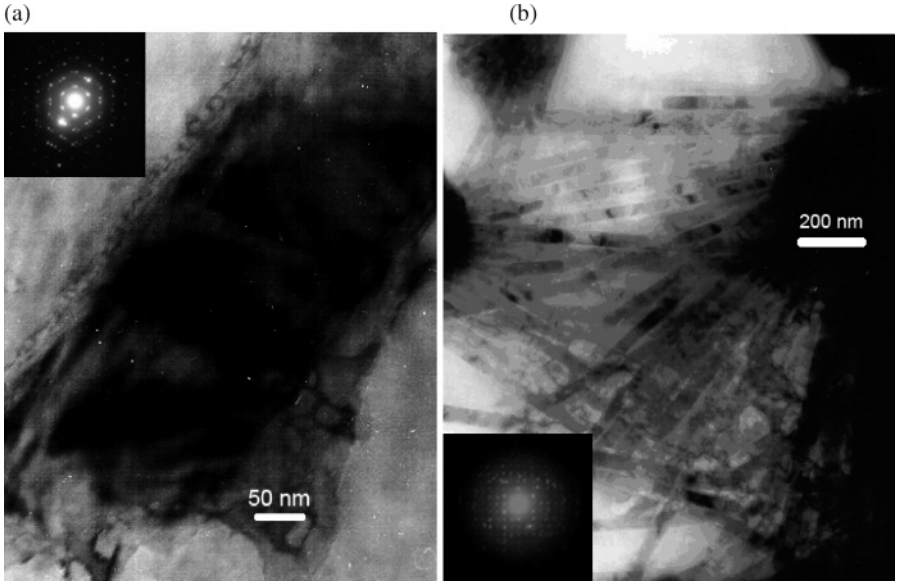

Figure 9. Crystalline structures formed from (a) 1-dodecene grafted silicon nanoparticles and (b) styrene-grafted silicon nanoparticles. The insets are selected area electron diffraction patterns (SAED). TEM grids were prepared by dropping a cyclohexane dispersion (0.13 mg/mL for dodecene-grafted particles, 0.15 mg/mL for styrene-grafted particles) onto a carbon-coated copper TEM grid and evaporating the solvent.

Supporting Information (Figures S16−S21). Quenching is not instantaneous but occurs on a time scale of minutes. Quenching was accompanied by a blue shift of the main PL emission as well as an 80−90% decrease in PL intensity. Both quenching and recovery by addition of TFA were accompanied by an increase in blue emission between 400 and 500 nm. The source of this blue emission cannot be established from the present results. Upon addition of TFA, an organic acid that protonates the triethylamine, partial recovery of the PL was observed. Additional studies, including time-resolved PL spectroscopy, will be required to achieve a more quantitative and mechanistic understanding of the PL quenching and recovery.

When styrene-grafted or 1-dodecene-grafted silicon particles were prepared for TEM imaging by casting a colloidal dispersion of them onto a carbon-coated copper TEM grid and evaporating the solvent, self-assembled crystalline structures were reproducibly observed. This appears to result from crystallization of the organic component of the grafted nanoparticles. The crystal structure was dependent on what molecule was grafted to the nanoparticle surface. Figure 9a shows a crystalline structure assembled from 1-dodecene grafted silicon nanoparticles. Figure 9b shows styrene-grafted silicon nanoparticles assembled into rodlike crystalline domains, roughly 45 nm in diameter. The SAED pattern in the inset of Figure 9a corresponds to a d spacing of about 2.14 Å with hexagonal symmetry. A different spot on the same sample, presumably corresponding to a different orientation of the same crystal structure, gave a distorted hexagonal pattern with d spacings of about 1.55, 1.84, and 2.03 Å. The SAED pattern in the inset of Figure 9b has a rectangular pattern corresponding to d spacings of about 6.1 and 6.5 Å. When the electron beam was focused on these structures, they rapidly melted. This is consistent with differential scanning calorimetry (DSC) measurements (Figure S22 in the Supporting Information) that showed an endothermic phase transition at 44.5 °C for dodecene-grafted silicon and 66 °C for styrene-grafted silicon. These transitions are about 80 and 97 °C above the normal melting points of 1-dodecene (mp = −35 °C) and styrene (mp = −31 °C), respectively. High-resolution images of the melted region confirmed that it contained silicon nanoparticles within it (Figure S23 in the Supporting Information). As discussed above, the mass fraction of silicon in the grafted particles is only about 30% for green-emitting nanoparticles with styrene or 1-dodecene on their surface. This corresponds to a silicon volume fraction of less than 15%. From this perspective, it is perhaps not surprising that the organic molecules can crystallize around the comparatively small silicon cores. The covalent attachment of the organic molecules to the silicon surface presumably restricts their movement and promotes crystallization.

Conclusions

In summary, we have developed an improved etching procedure to generate luminescent silicon nanocrystals with very high Si−H coverage and low oxygen content on their surface. This enables efficient (high coverage) grafting of various molecules containing a terminal double bond onto the particle surface via UV-initiated hydrosilylation reactions. The resulting covalently bound monolayers were able to protect the particles from chemical attack and partially protect them from PL quenching by triethylamine. The organic monolayer also allowed formation of stable nanoparticle dispersions in a variety of solvents. Chromatographic separation of particles by size was possible using these stable dispersions. Monomers including styrene, vinyl acetate, and ethyl undecylenate provide functional groups useful for carrying out further derivatization. Vinyl acetate and ethyl undecylenate grafted silicon can be hydrolyzed to generate alcohol and carboxylic acid functional groups. Reaction with 1-hexen-5-ol and undecanol directly provided an alcohol-functionalized surface. These functional groups can allow the further derivatization of the particles for use as reactive probes in bioimaging, in sensors, or for assembling nanoscale hybrid inorganic/organic semiconductor devices.

Supporting Information Available: Peak assignments for FTIR spectra of grafted silicon nanoparticles (Table S1); peak assignments for ^{1}H NMR spectra of grafted silicon nanoparticles (Table S2); FTIR spectra of etched particles after washing with water (Figure S1); high-resolution TEM of etched silicon nanoparticles (Figure S2); powder XRD spectra of

etched silicon nanoparticles (Figure S3); additional FTIR (Figure S5) and ^{1}H NMR (Figures S5 and S6) spectra of grafted silicon nanoparticles; TGA curves from grafted silicon nanoparticles (Figure S7); FTIR spectra demonstrating stability of grafted silicon nanoparticles against degradation by heating, UV illumination, and exposure to basic solutions (Figures S8−S15); PL spectra showing quenching by triethylamine and recovery of PL upon addition of trifluoroacetic acid (Figures S16−S21); DSC traces for grafted silicon nanoparticles (Figure S22); high-resolution TEM of structures shown in Figure 9, after beam-induced melting (Figure S23). This material is available free of charge via the Internet at http://pubs.acs.org.

LA0509394